Article ID: 1006-8775(2017) 02-0191-11

ANALYSIS OF "BIMODAL PATTERN" STORM ACTIVITY CHARACTERISTICS OF THE BAY OF BENGAL

DUAN Xu (段 旭)[1], DUAN Wei (段 玮)[1], LIN Zhi-qiang (林志强)[2]
(1. Yunnan Institute of Meteorology Sciences, Kunming 650034 China; 2. Meteorological Observatory of Tibet Autonomous Region, Lhasa 850000 China)

Abstract: Storms that occur at the Bay of Bengal (BoB) are of a bimodal pattern, which is different from that of the other sea areas. By using the NCEP, SST and JTWC data, the causes of the bimodal pattern storm activity of the BoB are diagnosed and analyzed in this paper. The result shows that the seasonal variation of general atmosphere circulation in East Asia has a regulating and controlling impact on the BoB storm activity, and the "bimodal period" of the storm activity corresponds exactly to the seasonal conversion period of atmospheric circulation. The minor wind speed of shear spring and autumn contributed to the storm, which was a crucial factor for the generation and occurrence of the "bimodal pattern" storm activity in the BoB. The analysis on sea surface temperature (SST) shows that the SSTs of all the year around in the BoB area meet the conditions required for the generation of tropical cyclones (TCs). However, the SSTs in the central area of the bay are higher than that of the surrounding areas in spring and autumn, which facilitates the occurrence of a "two-peak" storm activity pattern. The genesis potential index (GPI) quantifies and reflects the environmental conditions for the generation of the BoB storms. For GPI, the intense low-level vortex disturbance in the troposphere and high-humidity atmosphere are the sufficient conditions for storms, while large maximum wind velocity of the ground vortex radius and small vertical wind shear are the necessary conditions of storms.

Key words: storm of BoB; "bimodal pattern" activity characteristics; cause analysis; environmental conditions; GPI index
CLC number: P444 **Document code:** A
doi: 10.16555/j.1006-8775.2017.02.007

1 INTRODUCTION

Tropical cyclones (TCs), which are also known as the typhoon and hurricane, can cause catastrophes, thus having been a hot research topic in the meteorological field. The generation condition of TC is one of the key studies. Palmen pointed out that TC is formed only in sea areas with a surface temperature of above 26℃[1]. In fact, SST reflects the air-sea flux condition (Jiang et al.[2]). Gray[3] elevated the temperature threshold to 26.5℃, and pointed out that three thermal factors and three dynamic factors respectively affected the generation and development of TC. The dynamic factors are Coriolis force, low level relative vorticity and vertical wind shear, and the thermal factors are sea temperature, relative humidity and static stability. Chen et al.[4,5] believed that the basic conditions of TC are that the sea temperature is above 26℃, there is convergence in the low level or boundary layer, and the vertical wind shear (V200 hPa−V850 hPa) is less than 10 m/s. Zhu[6] believed that the necessary conditions for the generation and development of TC are that the sea surface temperature is higher than 26−27℃, the vertical wind shear in the troposphere is small and that there are effects by low-level initial disturbance and high-level divergence in the troposphere and certain Coriolis forces. He also pointed out that, on a global level, 65% of TCs occur within the 10−20°N area, 22% south of 10°N (mostly concentrated between 5−10°N), and 13% north of 20°N. Based on these previous achievements, Emanuel [7] and Nolan [8] proposed a genesis potential index (GPI) to quantitatively assess the generation conditions of TC, with consideration to the environmental factors that have significant influence on the generation of TC, such as sea surface temperature (SST), thermal uplift, high- and low-level vertical shear, humidity in the middle and low levels and absolute vorticity. For absolute vorticity, the larger the initial column integrates absolute vorticity, the greater the genesis efficiency is. Given the same column-integrated absolute vorticity, a bottom vortex has higher genesis efficiency than a mid-level vortex (Ge et al.[9]). Given the same column-integrated absolute vorticity, a bottom

Received 2015-10-08; **Revised** 2017-04-13; **Accepted** 2017-05-15
Foundation item: Meteorological Administration Special Public Welfare Research Fund of China (GYHY201106005); National Natural Science Foundation of China (41665004, 41205067)
Biography: DUAN Xu, Senior Engineer with the rank of professor, primarily undertaking meteorological research on Yunnan and its surrounding areas.
Corresponding author: DUAN Wei, e-mail: duanwain@hotmail.com

vortex has higher genesis efficiency than a mid-level one. GPI is a quantitative factor which may accurately represent the generation conditions of TC. GPI may accurately reflect the generation condition of TC, forecast the number of TC generated in each ocean, and judge the contributions of different environmental factors (Camargo[10-12]).

The Bay of Bengal (BoB) in the north Indian Ocean (NIO) is one of the regions where tropical cyclones (TCs) form frequently (Lin et al.[13]). A great number of studies have been carried out regarding the influences of storm activity in the BoB (Zhu et al.[14]; Yang et al.[15]; Xu et al.[16]; Zhang et al.[17]; Wang et al.[18]; Wang et al.[19]; Lv et al.[20]), but seldom has any cause analysis of the storm activity reported. In addition, the more important thing is that the tropical storm activity in the BoB shows a bimodal pattern (Li[21]; Wu[22]; Wang et al.[23]). The new data also confirmed the same characteristics (Duan et al.[24-26]). Namely, the two peak periods of storm activity in the BoB occurred in May and from October to November of every year. However, the tropical cyclone activity in other sea areas is unimodal and occurs in summer. Obviously, more analysis is needed for tropical cyclogenesis and environmental field over the BoB. Especially, for example, what causes the "bimodal pattern" storm activity characteristics?

In this manuscript we use Joint Typhoon Warning Center (JTWC) best-track data in conjunction with reanalysis data of the National Center for Environment Predictions (NCEP) and sea surface temperature (SST) of National Oceanic and Atmospheric Administration (NOAA). The above environmental conditions and genesis potential index (GPI) are used as references for the cause analysis of bimodal pattern storm activity in the BoB. The remainder of the manuscript is organized as follows. Section 2 describes the data and methods used in this study. Section 3 presents the climatological distribution of storm generation in the BoB. Section 4 discusses the climatological relation between the seasonal transition of environmental field and tropical cyclogenesis. Section 5 analyses the relation of storm generation number and GPI. Section 6 summarizes the characteristics of the environmental field responsible for the cyclogenesis over the BoB.

2 DATA AND METHODS

2.1 *Data*

The data used in this paper are all for the period of 1981–2010. For the samples of the storms in the BoB (which, according to the conventional reference in countries around the North Indian Ocean, is a general term for tropical storm <TS> and hurricane H1–H5), the data for the tropical cyclone path provided by the JTWC (Joint Typhoon Warning Centre) are applied. These data include the longitude and latitude information of the tropical cyclone path, minimum pressure in the center, and maximum wind velocity near the center for every 6 h. For the sea surface temperature information, the monthly average global 1° × 1° sea surface temperature data of NOAA_OI_SST_V2 provided are applied. For the pressure, temperature, wind and humidity of the atmosphere, as well as the calculation of diagnostic quantity, the reanalysis data of the monthly average 2.5° × 2.5° provided by NCEP/NCAR are applied.

2.2 *Methods*

The GPI calculation formula defined by Emanuel[7] is as follows:

$$\mathrm{GPI}=|10^5\eta|^{3/2}\left(\frac{\mathrm{H}}{50}\right)^3\left(\frac{V_{\mathrm{pot}}}{70}\right)^3(1+0.1V_{\mathrm{shear}})^{-2} \quad (1)$$

where η is the absolute vorticity (s^{-1}) of 850 hPa; H is the relative humidity (%) of 700 hPa; is maximum TC potential intensity (PI) defined by Emanuel, the maximum wind velocity ($m \cdot s^{-1}$) at the radius of the maximum wind velocity close to the ground; and V_{shear} is the vertical wind shear ($m \cdot s^{-1}$).

The expression of V_{pot} is as follows (Emanuel[7]):

$$V_{\mathrm{pot}}=C_p(T_s-T_o)\frac{T_s}{T_o}\frac{C_k}{C_D}(\ln\theta_e^*-\ln\theta_e) \quad (2)$$

In V_{pot} (PI) formula, C_p is the heat capacity at constant pressure, T_s is the ocean temperature, T_o the mean outflow temperature, C_k is the exchange coefficient for enthalpy, C_D is the drag coefficient, θ_e^* is the saturation equivalent potential temperature at ocean surface, and θ_e is the boundary layer equivalent potential temperature.

The expression of V_{shear} is as follows:

$$V_{\mathrm{shear}}=V_{200\mathrm{hPa}}-V_{850\mathrm{hPa}} \quad (3)$$

where 200 hPa and 850 hPa are respectively the wind velocities of 200 hPa and 850 hPa.

The calculation area of GPI is the BoB region (80–100°E, 0–20°N).

3 BASIC DISTRIBUTION OF STORM GENERATION IN THE BOB

According to the statistics for the period of 1981–2010 provided by the JTWC, during these 30 years a total of 102 storms have occurred in the BoB. Fig.1a shows the position of the storm at the initial stage (generally tropical depression, TD), as well as the position when the TD developed into a TS. It is clear that the position of the TS is in the north of the TD in the BoB region.

Figure 1b shows the monthly distribution of storms that occurred in the BoB. Although the temporal limit of the statistics is not exactly the same as that of other studies (Li[21]; Wu[22]; Wang[23]; Duan et al.[24-25]), the values show a clear "bimodal pattern", i.e. the peak periods of storm activity in the BoB occur in May and from October to November every year. From the distribution diagram, it may be seen that 78 storms

occurred in May and from October to November, occupying 76.5% of the total sample; no storms occur in February or August; 56.9% occur to the north of 10° N and 43.1% to the south of it; when the TD develops into TS, the position clearly moves to the north; 79.4% occur to the north of 10°N and 20.6% to the south of it; and most of the storms in the south occur in winter.

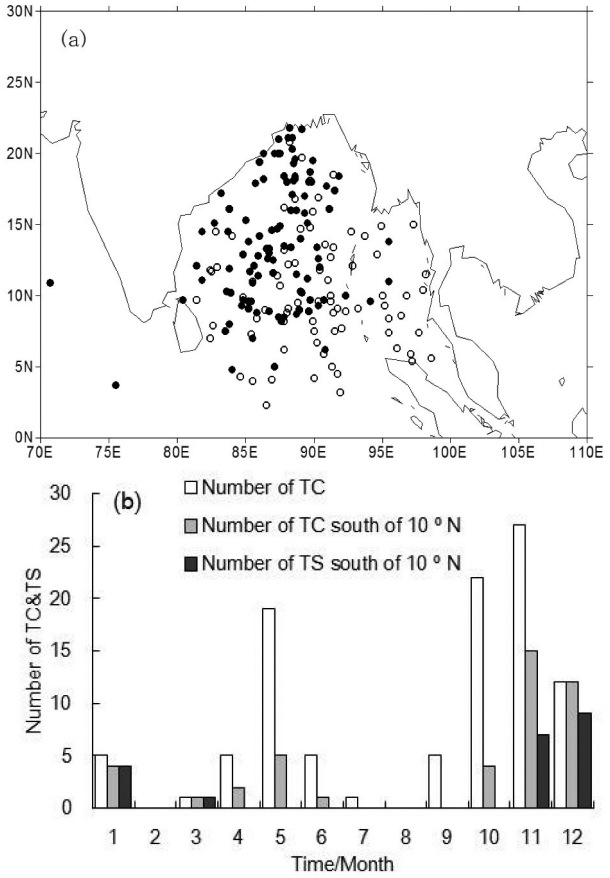

Figure 1. Spatial (a) and temporal (b) distribution of storms in the BoB from 1981 to 2010 ("○" represents the position of TC at the initial stage; "·" is the position of TS developed from TC).

4 ENVIRONMENTAL CONDITIONS OF STORM

4.1 *SST distribution*

Figure 2 shows the monthly average distribution of SST in the peak and valley months (the frequency of storm occurrence is zero) in the BoB region for the period of 1981–2010. In February, the SST distribution of SST in the BoB region tends to be low in the north and high in the south (Fig.2a). Except for the fact that the northernmost SST is lower than 26 ℃, most are higher than 26 ℃; the SSTs to the south of 15°N are higher than 27 ℃; and those to the south of 10°N are higher than 28 ℃; but there is basically no area with a temperature greater than 29 ℃. In May, the SST is the highest (Fig.2b). It is high in the central area, and relatively low in the northern and southern areas. The SST in the 10-15°N areas reaches 30 ℃; those to the north of 15°N and south of 10°N are all above 29.5 ℃. In August, the SSTs present a northwest-southeast trend (Fig.2c), i.e. the SSTs in the northwestern and southeastern areas are higher, at about 28.5–29 ℃; the other areas are lower, at about 28 –28.5 ℃. In November, the SST distribution is similar to that in May (Fig.2b). The central area is relatively high, at about 28.5–29 ℃ (Fig.2d); the SSTs in the north and south are low. Through this analysis, it is clear that the peak value of the storm activity is related to the high SST in the central area of the BoB.

From the above analysis, it is clear that the SST distribution of the BoB is high all through the year, which conforms to the necessary condition of TC (temperature above 26–27 ℃). Fig.3 shows the average SST distribution for each month in the BoB, which is similar to the "bimodal pattern" structure of storms. Despite the fact that from June to July and September the SSTs are higher than that from October to December, few storms are generated during the former period. This indicates that storms are affected by other conditions of the atmospheric environment (discussed later). On the other hand, the distribution type of the SST is possibly related to the "bimodal pattern" distribution of storms.

After further analysis, the SST distribution of the BoB can be generally divided into four types, possibly based on the occurrence frequency of storms. (1) The first distribution type is from December to April of the following year, when the SST decreases gradually from the south to the north (as in Fig.2a). In terms of SST, storms are more likely to occur in the south than in the north, but the generation of TC involves a certain Coriolis force, and the southern area is not conducive to the generation of storms. Therefore, the occurrence frequency of storms in these months is relatively low (Fig.1b). (2) The second distribution type occurs in May and November, when the central area of the BoB has a high SST, and the northern and southern areas have low ones. Thus May and November are the two peak months of the storm. Comparatively speaking, the high value range of SST in May occurs to the north of that in November (Figs.2b and 2d). The frequency of storms in November is higher than in May, the positions are clearly located in the south (Fig.1). (3) The third distribution type occurs from June to September, when the SST in the central area of the BoB is low, and the SSTs in the northern and southern areas are high (Fig.2c). This is clearly the last distribution which may lead to storms, as the higher SSTs are distributed in the positions unfavorable for the occurrence of storms, i.e. north and south. (4) The fourth distribution type occurs in October, where the SST in the BoB increases gradually from south to north (figure omitted). This is different from the second distribution, but considering that the northern area is unfavorable for the occurrence

of storms, this distribution type can be regarded as the same as the second type. Therefore, the occurrence frequency of storms in October is as high as that in May and November.

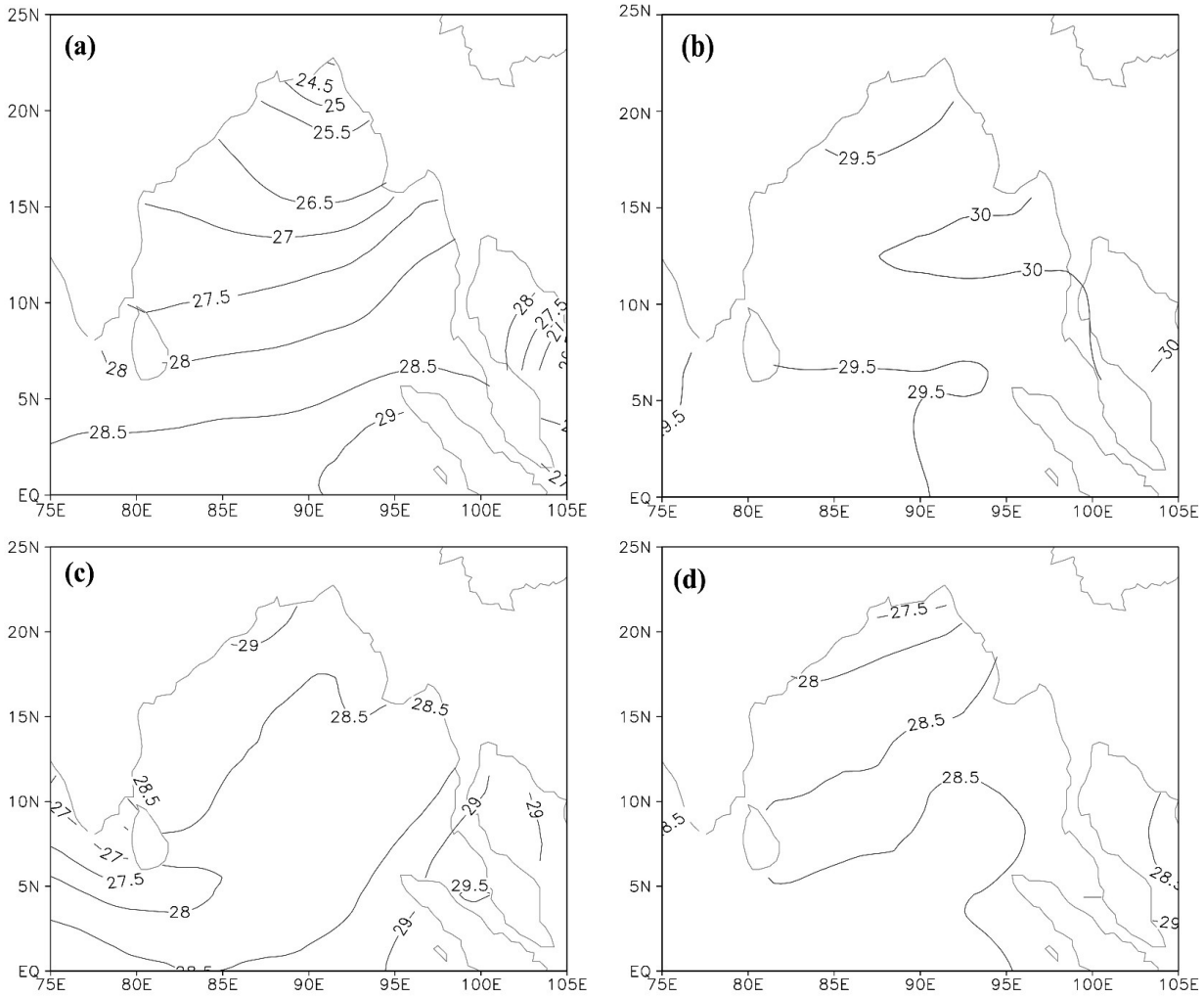

Figure 2. Monthly average SST distribution in peak and valley months in the BoB region for the period of 1981 to 2010 (unit: ℃). (a): February; (b) May; (c): August; (d): November.

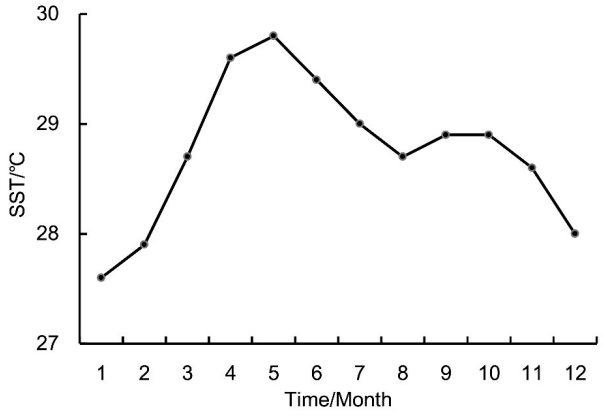

Figure 3. Monthly variation of SST in BoB region for the period of 1981 to 2010 (Average in sea areas: 80 to 100°E, 0 to 20°N, unit: ℃).

What needs attention is the phenomenon that, only from the sea surface temperature and its distribution analysis, May is more favorable time for tropical cyclogenesis than November. However, the fact is that the number of TC in November is higher than that in May. This further verifies that SST is only one of the factors for tropical cyclogenesis, a non-controlling factor.

4.2 *Vertical wind shear*

It is generally believed (Chen [4]; Zhu et al.[6]) that the vertical wind shear in the troposphere determines whether the latent heat released by the convective condensation of initial disturbance may be concentrated to a limited space. If the vertical wind shear in the troposphere is small, the relative movement of air at high and low level of troposphere will be infrequent. The latent heat of condensation produced by cumulus convection in tropical disturbance will intensively heat an air column in a limited space, which forms a warm-center structure rapidly. This guarantees a constant decrease in the pressure of initial disturbance

and eventually the formation of a storm. On the contrary, if the vertical wind shear is large and has good ventilation, the latent heat produced by cumulus convection will soon be whirled away from the disturbance area. Then the heat fails to be concentrated in a limited space, which hinders the formation of storms.

Figure 4 shows the monthly average distribution of V_{shear} in the peak and valley months in the BoB region for the period of 1981–2010. In February (Fig.4a), V_{shear} <10m·s^{-1} to the south of 10°N, which is conducive to the generation of storms. However, the low-latitude area close to the Equator is a barrier, thus there are no storms in February. The V_{shear} increases with the increase of latitude to the north of 10°N, which is unfavorable for the generation of storms. In May (Fig.4b), the low-value range of V_{shear} is in the northernmost area in a year. It is even less than 10 m·s^{-1} in the 10–22°N area and less than 5 m·s^{-1} in the 15–20°N area. The central and northern areas of the BoB are conducive to the generation of storms, and the occurrence frequency at these latitudes is high. These two favorable factors contribute to the peak value of the generation number of storms. In August (Fig.4c), in most areas of the BoB, the peak value is larger than 20 m·s^{-1}; to the south of 15°N, it is larger than 25 m·s^{-1}; and to the south of 10°N, it is larger than 30 m·s^{-1}. This is most unfavorable for the generation of storms. In November (Fig.4d), the distribution of V_{shear} is similar to that in May. However, the low-value range is found to the south of the central BoB, covering a larger area than in May. Therefore, November is the most favorable month for the generation of storms. Compared with May (Fig.4b), the small-value area of V_{shear} in November (Fig 4d) has the following characteristics: larger area, smaller value and more favorable position.

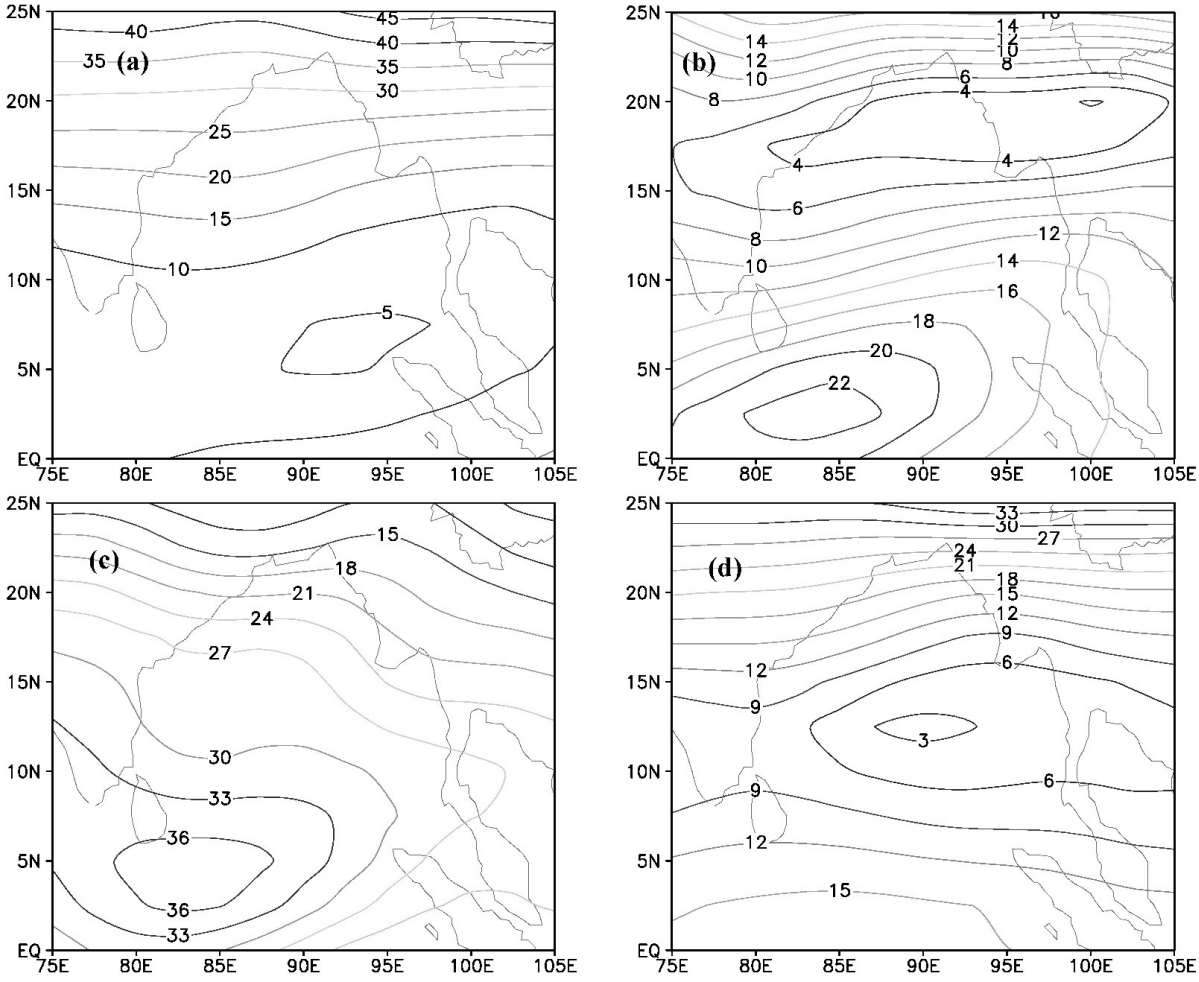

Figure 4. Monthly average distribution of V_{shear} in peak and valley months in the BoB region for the period of 1981—2010 (unit: m·s^{-1}). (a): February; (b) May; (c): August; (d): November.

The monthly variation of V_{shear} in the BoB region is quite large. From the perspective of the monthly average of the total area (80–100°E, 0–20°N) and the area in the north of 10°E (80–100°N, 10–20°E, see Fig.5), the monthly variation of V_{shear} is the highest from June to September, at more than 20 m·s^{-1}; and it is

smallest from April to May and from October to November, at less than 15 m·s^{-1}. The "double valley" months of V_{shear} correspond to the "double peak" months in Fig.1b. If only the area to the north of 10°N is taken into account, there is better correspondence. Moreover, the V_{shear} in May and from October to November are both smaller than 8 m·s^{-1}, and this favors the generation of storms.

4.3 *Low –level initial disturbance and high –level divergence in the troposphere*

Through the flow fluid analysis of the monthly averages of 850 hPa and 200 hPa (respectively representing the low and high levels of the troposphere) for the period of 1981–2010, the following observations may be made:

From January to April, the 850 hPa of the areas of the India Peninsula, the BoB and Indochina Peninsula is basically controlled by the subtropical high (Wang[27]); that of the area to the north of 20°N is controlled by the westerlies system; and that of the area to the south of 10° N is controlled by the equatorial convergence zone system (figure omitted). The 200 hPa of the area to the north of 15° N is controlled by the intense westerlies system; the South Asia high-pressure anticyclonic circulation is located in the south and east; the average ridge is near 10° N, with the westernmost point of the ridge to the east of 110° E from January to February, and extending to the place nearby from March to April (figure omitted). Clearly, the convergence disturbance in the low-level troposphere and the divergence in the high-level troposphere in the BoB and surrounding areas are not typical, which is unfavorable for the generation of storms.

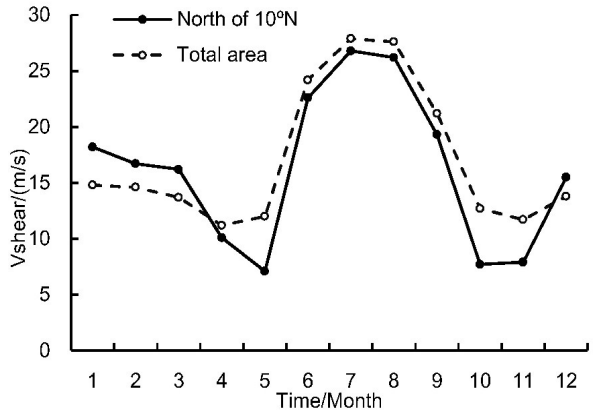

Figure 5. Monthly variation of average V_{shear} of the total area (80–100°E, 0–20°N) and area to the north of 10°N (80–100° N, 10–20° E) in the BoB region for the period of 1981–2010 (Unit: m·s^{-1}).

In May, with the establishment of the Somali cross-equatorial flow and its spread to the east, radical changes occur to the 850 hPa flow field of the BoB and Indochina Peninsula areas (Fig.6a, see Wang[27]; Qian[28]). The preceding east airflow changes to an intense southwest airflow, and there is a clear vortex convergence disturbance. The westerlies system of the 200 hPa withdraws to the north of 20°N, and the South Asia high-pressure anticyclonic circulation controls the Indochina Peninsula (Fig.6b). The South Asia High of 100 hPa is located in the northwest (figure omitted), and intense airflow divergence appears in the high level of the BoB. The circulation configuration of the convergence disturbance in the low-level troposphere and the divergence in the high-level troposphere favors the generation of storms.

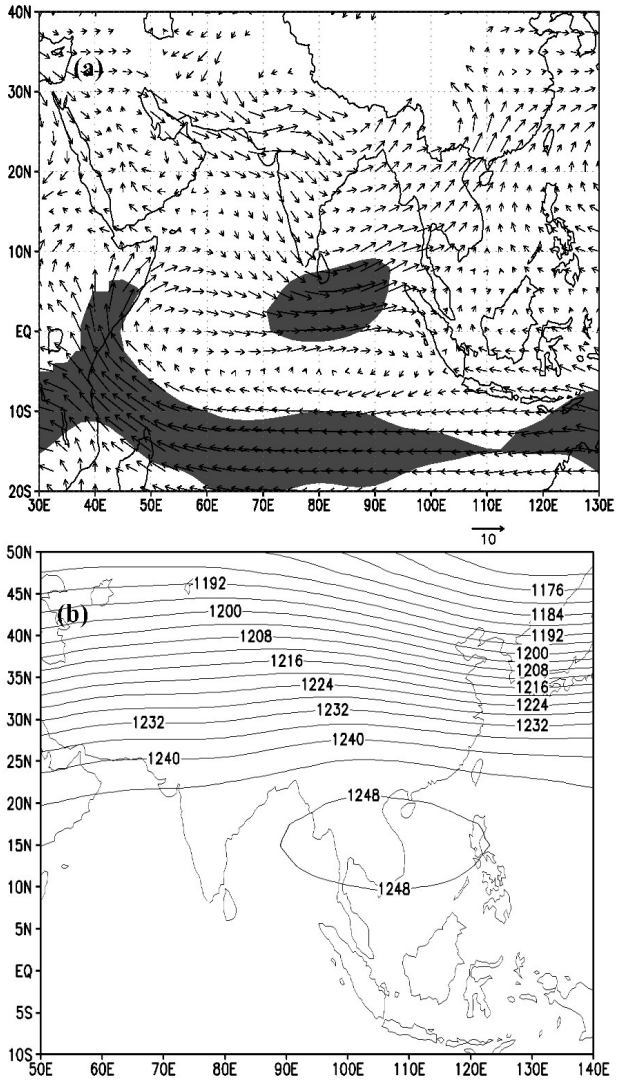

Figure 6. Monthly average flow field (shadowed area: wind velocity greater than 6 m·s^{-1}) and height field in May for the period of 1981 to 2010 (unit: m·s^{-1}, dagpm).

In June, the monsoon trough of 850 hPa in the BoB region continues to enhance (figure omitted), and clear convergence disturbance occurs (Wang[27]; Ding[29]). However, the South Asia High of 200 hPa continues to move to the north of India, Bangladesh and southern Tibetan Plateau (figure omitted). At the same time, the high-level airflow divergence in the BoB region

diminishes. The circulation configuration between the high and low levels hinders the generation of storms.

From July to August, the monsoon low in the BoB region develops to the peak (Wang[27]; Qian[28]; Ding[29]), and clear convergence disturbance occurs (Fig.7a). At this time, the South Asia High moves northward to the Iranian Plateau and Tibetan Plateau (Fig.7b). Although there is an intense vortex disturbance in the low-level troposphere, the center of airflow divergence in the high-level is located above the plateau. The high-level above the BoB region lacks the driving force to develop the vortex disturbance intensely and vertically in the low-level.

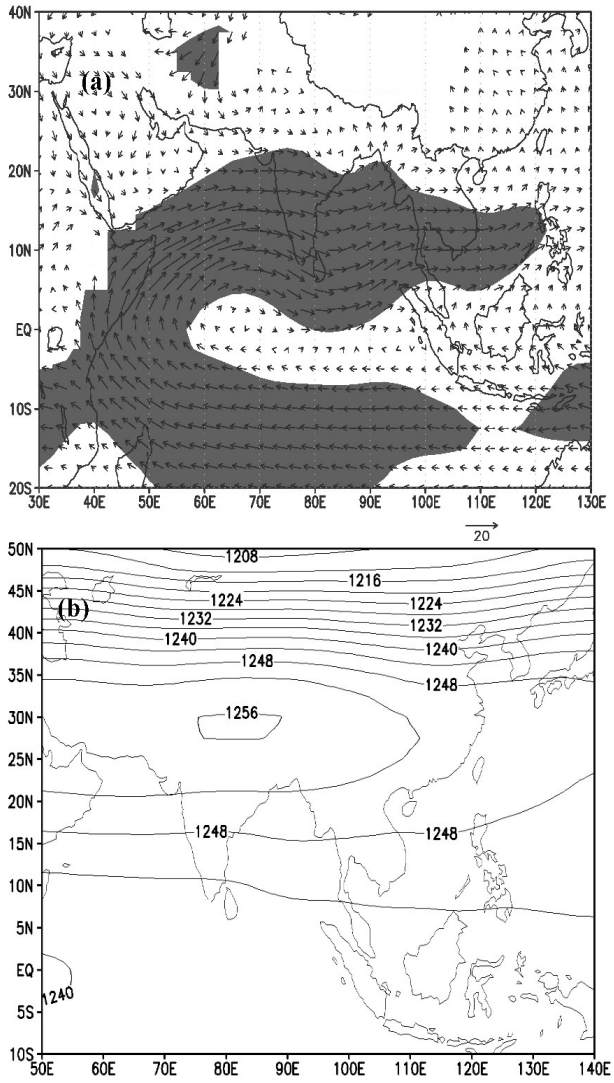

Figure 7. Monthly average flow field (shadowed area: wind velocity greater than 6 m·s^{-1}) and height field in August for the period of 1981 to 2010 (unit: m·s^{-1}, dagpm).

In September, the southwest monsoon of 850 hPa begins to diminish but remains strong in convergence disturbance (figure omitted, see Wang[27]; Qian[28]). The South Asia High of 200 hPa begins to withdraw from the plateau and control the northern India, Bangladesh and southern Tibetan Plateau areas (figure omitted). The circulation configuration between the high- and low-levels is similar to that in June. The high-level divergence in the north of the BoB region enhances and favors the generation of storms. However, in the southern and central areas, it is unfavorable for the generation of storms.

In October, the southwest monsoon of 850 hPa weakens sharply (Wang[27]). The East Asian summer monsoon begins to withdraw to the south and controls the northern area of the Indochina Peninsula. The two weakening monsoons meet near 100°E (figure omitted), and the superimposed effect retains a strong divergence disturbance in the BoB region. The South Asia High of 200 hPa withdraws to the India Peninsula, BoB and Indochina Peninsula. Therefore, the circulation patterns of high-level divergence and low-level convergence in the BoB region are formed once again, which favors the formation of storms.

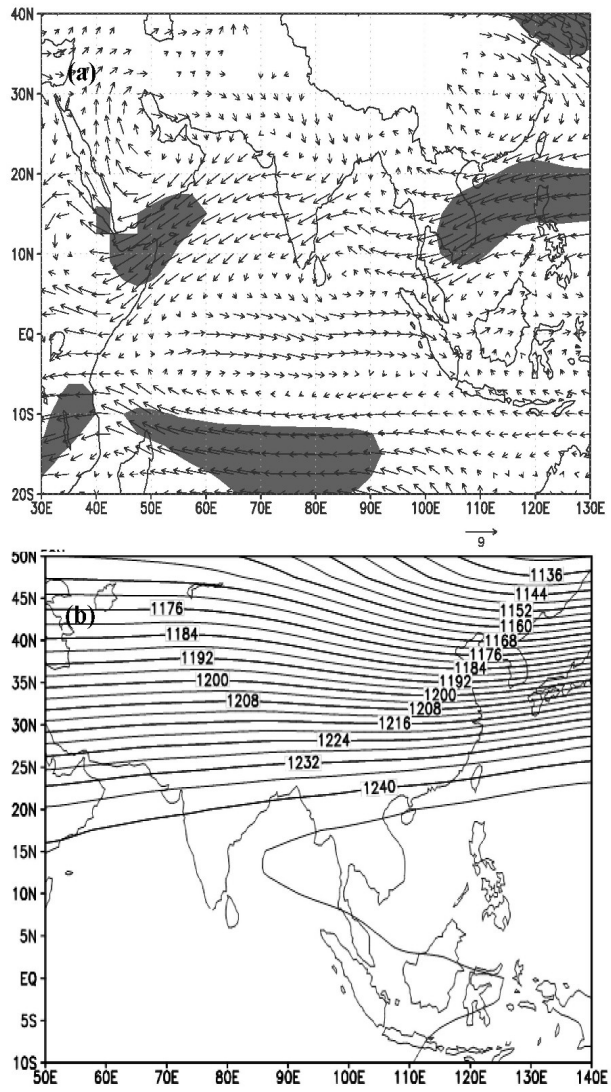

Figure 8. Monthly average flow field (shadowed area: wind velocity larger than 6 m·s^{-1}) and height field in November for the period of 1981 to 2010 (unit: m·s^{-1}, dagpm).

In November, the southwest monsoon in the BoB region of 850 hPa is completely replaced by the southeast monsoon (Fig.8a, see Wang [27]). Since the position is in the north and the wind velocity is high, intense convergence disturbance still remains. The anticyclonic circulation of 200 hPa continues to withdraw to the southeast, but it still controls the BoB and Indochina Peninsula (Fig.8b). There is still intense airflow over the central and southern areas of the BoB. In addition, there is intense divergence in the high-level and strong convergence in the low-level. This is conducive to the generation of storms.

In December, the equatorial convergence zone of 850 hPa withdraws to the south of 10° N (figure omitted), and the convergence disturbance in the BoB region clearly weakens (especially in the central and northern areas). The anticyclonic circulation of 200 hPa continues to withdraw to the southeast until reaching the Indochina Peninsula (figure omitted). The high-level divergence and low-level convergence in the central and northern areas of the BoB are both weak, which hinders the generation of storms. The southern area still remains in the stage of high-level divergence and low-level convergence, which favors the generation of storms.

5 RELATION OF STORM GENERATION NUMBER AND GPI

Using Eq.(1), the average GPI of the range (80–100° N, 0–20° E) is calculated. When analyzing the relation between the GPI and the factors it contains and the number of storms (NS), the data is homogenized, as the units and dimensions are different and inconvenient for comparison. The homogenization of the data is calculated as follows:

$$X_i=\frac{x_i-x_{\min}}{x_{\max}-x_{\min}} \quad (4)$$

where X_i is the datum after the homogenization; x_i, $x_{\max}$ and $x_{\min}$ are respectively the raw datum, and maximum and minimum values of the raw data sequence, i=1, 2, …,12 (month).

In Fig.9, the monthly average GPI and monthly variation of NS in the BoB region are provided. It can be seen that there is a clear correspondence between the two variables, and the "bimodal pattern" characteristic of GPI is consistent with NS. Just during December to the following January, the two variable trends are slightly different. The cause is that the position of the storms is in the south of the BoB (Fig.1b) in the two months, but the GPI is the average value for the entire BoB region.

Wu once used the "multi-voting" method to quantitatively analyze the cause of the bimodal pattern storm of the BoB based on the seasonal variation of equatorial airflow, ITCZ, south branch of the westerly tough, western Pacific Subtropical High, and South Asia High [22]. Due to data limitations, there has been no quantitative analysis on the atmospheric elements and SST. In Eq.(1), the four constituting factors of GPI, η, and V_{pot} are in direct proportion, and V_{shear} is in inverse proportion. Fig.10 provides the monthly variations of η, H, V_{pot} and V_{shear} for the variation of NS in the BoB region from 1981 to 2010. Their relationship is quantitatively analyzed in the following section.

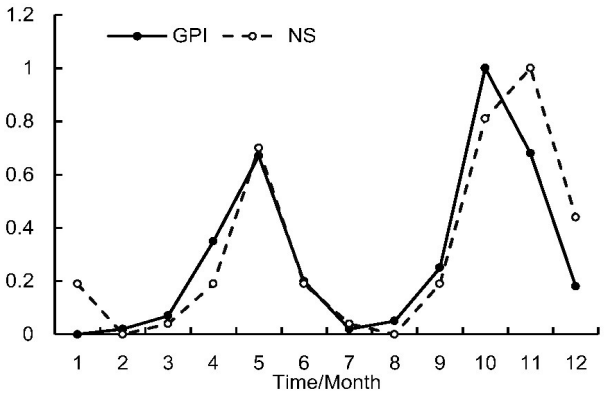

Figure 9. Monthly average GPI and NS (homogenized data) distribution in the BoB region (80–100°E, 0–20°N) for the period of 1981 to 2010.

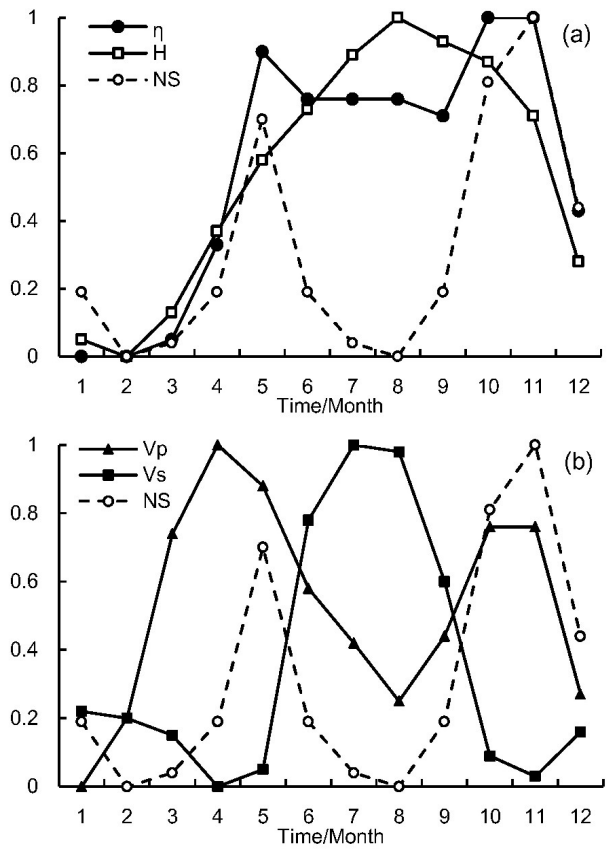

Figure 10. Monthly average GPI items and NS (homogenized data) distribution in the BoB region (80–100°N, 0–20°E) for the period of 1981 to 2010 (Vp meas V_{pot},Vs means V_{shear}).

The values of η (absolute vorticity: 850 hPa) in summer and autumn are clearly higher than in winter and spring. This is significantly affected by seasonal change. In summer and autumn, the equatorial

convergence zone system is located in the north, and in the BoB region the monsoon low is active. In winter and spring, the westerlies system is located in the south, and the BoB region is controlled by the subtropical high. The intensity of η in the low level of the troposphere is determined by this situaton. However, the η still has two peak values in May and from October to November (which may be related to the outburst and weakening of the monsoon), which is consistent with the peak values of NS and positively contributes to the "bimodal pattern" structure of the GPI. If the factor η is used alone in the measurement, storms may occur all through May to November.

The variation of H (relative humidity of 700 hPa) is smallest in February. It rises from March to July and reaches its highest point in August, and then it reduces gradually month by month until reaching its minimum value in February. This is different from the NS in the "bimodal pattern" structure. From the second item of Eq.(1), it can be seen that, when >50%, the item is larger than 1; otherwise, it is smaller than 1. Its third power has a great influence on the GPI. Due to the fact that the raw data of H from December to March of the following year are smaller than 50%, those from May to November are 50%. Therefore, the contribution of H from May to November and from December to the following March either increases or decreases sharply. Clearly, the high humidity in the low level troposphere, namely the humidity field from May to November, especially from July to October, favors the generation of storms.

The distribution of V_{pot} (maximum wind velocity at the radius of maximum wind velocity close to the ground) also shows a "bimodal pattern" structure, which is basically consistent with NS. From the third item of Eq.(1), it can be seen that when V_{pot}>70 m·s^{-1}, the item is larger than 1; otherwise, it is smaller than 1. Its third power also has a great influence on the GPI. The raw data of V_{pot} from December to February of the following year and from July to September are smaller than 70 m·s^{-1}; those from March to June and from October to November are larger than 70 m·s^{-1}. This is basically the same as the variation distribution of NS, and it may be deduced that a large V_{pot} favors the generation of storms.

The V_{shear} (vertical wind shear) is exactly opposite to the "bimodal pattern" structure of the GPI and NS, showing an "inverse bimodal pattern". From the fourth item of Eq. (1), it can be seen that the larger the V_{shear} is, the smaller the GPI is. The period of June to September is the most unfavorable time for the generation of storms; from April to May and from October to November are the most favorable times for the generation of storms.

6 SUMMARY AND DISCUSSION

In this paper, through the analysis of atmospheric environmental field and genesis potential index (GPI) in the BoB and surrounding areas, the generation conditions of storms in the BoB and the "bimodal pattern" distribution caused by superimposed effects of advantageous conditions are further studied.

(1) The SSTs in the BoB region are high all the year round, which conforms to the necessary conditions of TC. It is known from comparison analysis that the SSTs in the central area of the BoB in May and from October to November are higher than those in the surrounding areas. This coincides with that of the global sea areas (10–20°N) with the highest incidence of TC. In April, with higher SST, the SSTs tend to be high in the south and low in the north. From June to September, the SSTs are lower in the surrounding areas than in the central areas. The high SSTs are located in either the north or south, where the occurrence frequency of storms is low. This indicates that the higher SSTs in the central area of the BoB than that of its surroundings is one of the causes of the "bimodal pattern" distribution of storms.

(2) The distribution of V_{shear} has a good corresponding relationship with NS. The peak (valley) distribution of NS is almost the same as the valley (peak) of V_{shear}, which indicates that the accumulation and diffusion of heat inside the troposphere is crucial to the generation of storms. This also indicates that the accumulation intensity of the "bimodal pattern" months is clearly higher than that in other months.

(3) The convergence disturbance in the lower-level troposphere in the BoB region is strong in all months, except being weakest during January to April and weaker in December. It is strongest from June to August, which seems to have no close relation to the "bimodal pattern" distribution of storms, and may even be opposite to it. However, in addition to convergence disturbance in the low-level, a strong divergence in the upper-level is also required, which contributes to the formation of vortex air column by propelling the low-level airflow to the high-level, while dispersing the high-level airflow. The atmospheric circulation in the high-level troposphere varies depending on the season. The high-level anticyclonic circulation (called the South Asia High when larger than 100 hPa) representing the airflow divergence in the East Asia area swings in the northwest-southeast direction. In May and from October to December, the circulation swings to the high level of the BoB and Indochina Peninsula, and coordinating with the convergence disturbance in the low-level, it contributes to the favorable conditions of the vortex air column. From July to August, when the convergence disturbance in the low-level is the strongest, the anticyclonic circulation in the high-level moves northward to the Iranian Plateau and Tibetan Plateau. There is no intense air divergence found north of the BoB region, which hinders the formation of the vortex air column. Therefore, it is believed that the seasonal

variation of atmospheric circulation in the East Asia area leads to the "bimodal pattern" distribution of storms, since the conversion periods of winter and summer circulations are exactly in the same periods of May and October to November.

(4) The GPI is linked with the atmospheric element fields relating to occurrence of TC, which comprehensively reflects the potential conditions for generation of TC. It also accurately represents the "bimodal pattern" distribution of the BoB storms. Through analysis of the items of the GPI in the BoB region it can be seen that the intense vortex disturbance in the low-level troposphere and the high-humidity atmosphere are the sufficient conditions for storms, while large maximum wind velocity of the ground vortex radius and small vertical wind shear are the necessary conditions of storms. Therefore, the "bimodal pattern" distribution of storms is mainly determined by the latter two conditions.

(5) The bimodal pattern storm activity of the BoB is result of multiple factors. In two peak periods (May and October—November), the SSTs in the central area are higher than that of the surrounding areas and the northern of the BoB, and small vertical wind shear, the vortex disturbance in the lower-level troposphere and the high-humidity atmosphere, the divergence of anticyclonic circulation also appear in this area. However, there is no such phenomenon in other time periods.

REFERENCES:

[1] PALMEN E H. On the formation and structure of tropical cyclones [J]. Geophys, 948, 3: 26-28.

[2] JIANG Di, HUANG Fei, HAO Guang-hua, et al. The characteristics of air-sea heat flux exchange during the Generation and development of local typhoons over the South China Sea [J]. J Trop Meteorol, 2014, 20 (2): 93-102.

[3] GRAY W M. Environmental influences on tropical cyclones [J]. Austr Meteorol Mag, 1988, 36(3): 127-139.

[4] CHEN Lian-shou, DING Yi-hui. Introduction of the Western Pacific Typhoon [M]. Science Press, 1979: 105-108 (in Chinese).

[5] CHEN Lian-shou, DING Yi-hui, LUO Zhe-xian, et al. The Introduction of Tropical Cyclone Dynamics [M]. China Meteorological Press, 2002: 310-313 (in Chinese).

[6] ZHU Qian-gen, LIN Jin-rui, SHOU Shao-wen,et al. The Pinciple and Method of Weather (4th ed) [M]. China Meteorological Press, 2007: 508-554 (in Chinese).

[7] EMANUEL K A. An air-sea interaction theory for tropical cyclones, Part I: steady-state maintenance [J]. J Atmos Sci, 1986, 43(4): 585-604.

[8] NOLAN D S, ERIC D R, EMANUEL K A. Tropical cyclogenesis sensitivity to environmental parameters in radiative-convective equilibrium [J]. Quart J Roy Meteorol Soc, 2007, 133(10): 2085-2107.

[9] GE Xu-yang, LI Tian-ming, PEN Shun-tai. Tropical cyclone genesis efficiency: mid-level versus bottom vortex [J]. J Trop Meteorol, 2013, 19(3): 197-213.

[10] CAMARGO S J, SOBEL A H, BAMSTON A G, et al. Tropical cyclone genesis potential index in climate models [J]. Tellus, 2007, 57A(4): 428-443.

[11] CAMARGO S J, EMANUEL K A, SOBEL A H. Use of a Genesis Potential Index to Diagnose ENSO Effects on Tropical cyclone Genesis [J]. J Climate, 2007, 20(10): 4819-4834.

[12] CAMARGO S J, WHEELER M C, SOBEL A H. Diagnosis of the MJO modulation of tropical cyclogenesis using an empirical index [J]. J Atmos Sci, 2009, 66(10): 3061-3074.

[13] LIN Zhi-qiang, BIANBA Zha-xi, WEN Sheng-jun, et al. Objective classification of the tracks of tropical storms in the Bay of Bengal [J]. J Trop Meteorol, 2015, 21(3): 222-231.

[14] ZHU Fu-kang, ZHENG Xin-jiang, LUO Jing-ning, et al. Water vapor image of snowstorm process in Southern Tibet [J]. Chin Sci Bull, 2011, 43(20): 2232-2235.

[15] YANG Zu-fang, LI Yue-an, LI Wei-hua. Comparative analysis of the different effects of two Bay of Bengal storms on precipitation in China [J]. Marine Forecast, 2000, 17(4): 41-46 (in Chinese).

[16] XU Mei-ling, DUAN Xu, ZHANG Xiu-nian. Numerical simulation of structural evolution of a landfalling over the Bay of Bengal storm [J]. Plateau Meteorol, 2006, 25(6): 1139-1146 (in Chinese).

[17] ZHANG Teng-fei, DUAN Xu, ZHANG Jie. Mesoscale analysis of Yunnan successive heavy precipitation caused by storms over the Bay of Bengal in the early summer [J]. J Trop Meteorol, 2006, 22(1): 67-73 (in Chinese).

[18] WANG Zi-qian, ZHU Wei-jun, DUAN An-min. A case study of snowstorm in Tibetan Plateau induced by Bay of Bengal storm: Based on the theory of slantwise vorticity development [J]. Plateau Meteorol, 2010, 29(3): 703-711 (in Chinese).

[19] WANG Man, DUAN Xu, Li Hua-hong, et al. A sensitivity experiment to the orographic effect on the Bengal storm of Mala during its landing [J]. Acta Meteorol Sinica, 2011, 69(3): 486-495 (in Chinese).

[20] LV Ai-min, WEN Yong-ren, Li Ying. Study of the impact of tropical cyclone Akash (0701) over the Bay of Bengal on a heavy rainfall event in Southwest China [J]. Chin J Atmos Sci, 2013, 37(1): 160-170 (in Chinese).

[21] LI Yu-zhu. Some features of the early summer storm over the Bay of Bengal [J]. Meteorol Mon, 1981, 7(5): 13-22 (in Chinese).

[22] WU Heng-qiang. Cause analysis of the bimodal period of storm activity characteristics of the BOB [J]. Meteorol Mon, 1986, 12(12): 6-8 (in Chinese).

[23] WANG You-heng, WANG Su-xian. A preliminary study of tropical cyclone over the Bay of Bengal [J]. Plateau Meteorol, 1988, 14(6): 19-22 (in Chinese).

[24] DUAN Xu, TAO Yun, CUN Canqiong,et al. Temporal and spatial distributions of storms over the Bay of Bengal and its activity characteristic [J]. Plateau Meteorol, 2009, 28(3): 634-641 (in Chinese).

[25] DUAN Xu, XU Mei-ling, QI Ming-hui: The Manual of Weather Forecaster of Yunnan Province [J]. China Meteorological Press, 2011: 84-96.

[26] DUAN Xu, DUAN Wei. Impact of Storms over the Bay of Bengal on Precipitation over Plateau area [J]. Plateau Meteorol, 2015, 34(1): 1-10 (in Chinese).

[27] WANG Bin. The Asian Monsoon [M]. Springer-Praxis Books in Environmental Sciences Press, 2006: 120-148.
[28] QIAN Wei-hong, DING Ting, TANG Shuai-qi. Some Understanding of the Seasonal March of Asian Monsoons [J]. J Trop Meteorol, 2010, 26(1): 111-116 (in Chinese).
[29] DING Yi-hui, JOHNNY C L C. The East Asian summer monsoon: an overview [J]. Meteorol Atmos Phys, 2005, 89(1-4): 117-142.

Citation: DUAN Xu, DUAN Wei and LIN Zhi-qiang. Analysis of "bimodal pattern" storm activity characteristics of the Bay of Bengal [J]. J Trop Meteorol, 2017, 23(2): 191-201.